Neuropharmacology 126 (2017) 12–24

Contents lists available at ScienceDirect

Neuropharmacology

journal homepage: www.elsevier.com/locate/neuropharm

Substantial protection against MPTP-associated Parkinson's neurotoxicity *in vitro* and *in vivo* by anti-cancer agent SU4312 via activation of MEF2D and inhibition of MAO-B

Baojian Guo [a, 1], Shengquan Hu [a, b, 1], Chengyou Zheng [a], Hongyu Wang [a], Fangcheng Luo [a], Haitao Li [c], Wei Cui [d], Xifei Yang [e], Guozhen Cui [f], Shinghung Mak [b], Tony Chung-Lit Choi [b], Edmond Dik-Lung Ma [g], Yuqiang Wang [a], Simon Ming Yuen Lee [c], Zaijun Zhang [a, *], Yifan Han [b, **]

[a] *Institute of New Drug Research and Guangzhou Key Laboratory of Innovative Chemical Drug Research in Cardio-cerebrovascular Diseases, Jinan University College of Pharmacy, Guangzhou, China*
[b] *Department of Applied Biology and Chemical Technology, Institute of Modern Chinese Medicine, The Hong Kong Polytechnic University, Hung Hom, Hong Kong, China*
[c] *State Key Laboratory of Quality Research of Chinese Medicine and Institute of Chinese Medical Sciences, University of Macau, Taipa, Macao, China*
[d] *School of Medicine, Ningbo University, Zhejiang, China*
[e] *Key Laboratory of Modern Toxicology of Shenzhen, Centre for Disease Control and Prevention, Shenzhen, China*
[f] *Department of Bioengineering, Zunyi Medical University, Zhuhai Campus, Zhuhai, China*
[g] *Department of Chemistry, Hong Kong Baptist University, Hong Kong, China*

A R T I C L E I N F O

Article history:
Received 8 November 2016
Received in revised form
25 July 2017
Accepted 10 August 2017
Available online 12 August 2017

Keywords:
Parkinson's disease
SU4312
Neuroprotection
Myocyte enhancer factor 2D
Monoamine oxidase-B

A B S T R A C T

We have previously demonstrated the unexpected neuroprotection of the anti-cancer agent SU4312 in cellular models associated with Parkinson's disease (PD). However, the precise mechanisms underlying its neuroprotection are still unknown, and the effects of SU4312 on rodent models of PD have not been characterized. In the current study, we found that the protection of SU4312 against 1-methyl-4-phenylpyridinium ion (MPP^+)-induced neurotoxicity in PC12 cells was achieved through the activation of transcription factor myocyte enhancer factor 2D (MEF2D), as evidenced by the fact that SU4312 stimulated myocyte enhancer factor 2 (MEF2) transcriptional activity and prevented the inhibition of MEF2D protein expression caused by MPP^+, and that short hairpin RNA (ShRNA)-mediated knockdown of MEF2D significantly abolished the neuroprotection of SU4312. Additionally, Western blotting analysis revealed that SU4312 potentiated pro-survival PI3-K/Akt pathway to down-regulate MEF2D inhibitor glycogen synthase kinase-3beta (GSK3β). Furthermore, using the *in vivo* PD model of C57BL/6 mice insulted with 1-methyl-4-phenyl-1,2,3,6-tetrahydropyridine (MPTP), we found that intragastrical administration of SU4312 (0.2 and 1 mg/kg) greatly ameliorated Parkinsonian motor defects, and restored protein levels of MEF2D, phosphorylated-Ser473-Akt and phosphorylated-Ser9-GSK3β. Meanwhile, SU4312 effectively reversed the decrease in protein expression of tyrosine hydroxylase in substantia nigra pars compacta dopaminergic neurons, inhibited oxidative stress, maintained mitochondrial biogenesis and partially prevented the depletion of dopamine and its metabolites. Very encouragingly, SU4312 was able to selectively inhibit monoamine oxidase-B (MAO-B) activity both *in vitro* and *in vivo*, with an IC_{50} value of 0.2 μM. These findings suggest that SU4312 provides therapeutic benefits in cellular and animal models of PD, possibly through multiple mechanisms including enhancement of MEF2D

Abbreviations: AD, Alzheimer's disease; CDKs, cyclin-dependent kinases; DMEM, Dulbecco's modified Eagle's medium; FBS, fetal bovine serum; GSK3β, glycogen synthase kinase 3β; MAO-B, monoamine oxidase-B; MEF2, myocyte enhancer factor 2; MPP^+, 1-methyl-4-phenylpyridinium ion; MPTP, 1-methyl-4-phenyl-1,2,3,6-tetrahydropyridine; PBS, phosphate buffered saline; PD, Parkinson's disease; ShRNA, short hairpin RNA; SNpc, substantial nigra pars compacta; SU4312, 3-[4-(dimethylamino)benzylidenyl] indolin-2-one; TH, tyrosine hydroxylase.

* Corresponding author. Institute of New Drug Research, Jinan University College of Pharmacy, Huangpu Road, Guangzhou, China.
** Corresponding author. Department of Applied Biology and Chemical Technology, Institute of Modern Chinese Medicine, The Hong Kong Polytechnic University, Hung Hom, Hong Kong, China.
E-mail addresses: zaijunzhang@163.com (Z. Zhang), bcyfhan@polyu.edu.hk (Y. Han).
[1] Contributed equally to this work.

http://dx.doi.org/10.1016/j.neuropharm.2017.08.014

through the activation of PI3-K/Akt pathway, maintenance of mitochondrial biogenesis and inhibition of MAO-B activity. SU4312 thus may be an effective drug candidate for the prevention or even modification of the pathological processes of PD.

1. Introduction

Parkinson's disease (PD) is the second most common neurodegenerative disorder, coming only next to Alzheimer's disease (AD), and it occurs in 2% of adults aged over 65. PD is primarily characterized by progressive dopaminergic (DA) neuronal loss in the substantia nigra pars compacta (SNpc) (Qiao et al., 2017; Tieu, 2011). Despite decades of research, the precise cause of PD is still unknown and further investigation of molecular mechanisms as well as identification of neuroprotective molecules remain indispensable. Currently available pharmacological interventions for PD, such as dopamine precursor, dopamine agonists, and monoamine oxidase (MAO) and catechol-*O*-methyltransferase inhibitors, could offer transient and limited benefits but without any disease-modifying potential, as they could not delay or stop the progressive loss of DA neurons. Therefore, it is generally accepted that effective drugs for PD treatment should address dopaminergic neuroprotection to reduce premature/mature neurodegeneration in addition to enhancing dopaminergic neurotransmission (Cacabelos, 2017).

Monoamine oxidase-B (MAO-B) inhibitors were originally designed to control PD symptoms by blocking the degradation of dopamine. Very encouragingly, studies in recent years have shown that selegiline and rasagiline, two FDA-approved irreversible MAO-B inhibitors, provide neuroprotective effects in a variety of *in vitro* and *in vivo* models associated with PD through MAO-B inhibition-independent mechanisms (Boll et al., 2011; Hara et al., 2006; Weinreb et al., 2010). For example, selegiline was able to protect cultured dopaminergic neurons against 1-methyl-4-phenylpyridine (MPP^+) through its anti-oxidant activity (Wu et al., 2000). More prominently, rasagiline induced an *in vivo* neurorestorative activity in SNpc neurons through the activation of tyrosine kinase receptor signaling pathway when given post-*N*-methyl-4-phenyl-1,2,3,6-tetrahydropyridine (MPTP) (Sagi et al., 2007). However, most efforts over the decades have failed to establish substantial neuroprotective interventions as true therapeutics that are able to delay PD progression, because no genuine novel therapeutic targets key to DA neuronal survival and new molecules have been identified (Rascol et al., 2011).

Myocyte enhancer factor 2 (MEF2) proteins are a family of transcription factors that consist of four distinct vertebrate isoforms, namely MEF2A, 2B, 2C and 2D. Though originally identified in muscle cells, these four MEF2 genes are widely distributed in the central nervous system (CNS) (Rashid et al., 2014). Accumulating lines of evidence have indicated that MEF2 genes, particularly MEF2D, play a vital role in neuronal survival in various experiment paradigms associated with PD (Chen et al., 2016; Huang et al., 2016; Smith et al., 2006; Yang et al., 2009), and that a number of death signal-related pathways including oxidative stress and glycogen synthase kinase-3beta (GSK3β) exhibit their inhibitory activities on MEF2D (Chen et al., 2016; Mount et al., 2013; Smith et al., 2006). For instance, neurotoxins related to PD, including α-synuclein, MPP^+ and MPTP reduced nigral MEF2D in experimental and/or idiopathic PD, and alterations of MEF2D correlated well with changes in tyrosine hydroxylase (TH, a marker for DA neurons) expression (Chu et al., 2011; Yao et al., 2012). Mechanistic studies further revealed that enhancing MEF2D in SNpc DA neurons was an important underlying mechanism in antagonizing neurotoxic events observed in such pathological conditions (She et al., 2011; Smith et al., 2006). These results strongly suggest that MEF2D represents a promising and effective therapeutic target for preventing and treating PD.

Many epidemiological studies support a general inverse association between cancer and age-related neurodegenerative diseases, particularly PD and AD (Driver, 2014; Musicco et al., 2013; Tabares-Seisdedos and Rubenstein, 2013). It has been reported that cancer survivors have a 20–50% lower risk of developing PD and AD, and patients with these neurological conditions have a substantially lower incidence of cancer (Driver, 2014). Potential biological explanations imply that there may be some common pathophysiological mechanisms such as mitochondrial dysfunction and oxidative stress that drive both conditions (Driver, 2014). There is evidence suggesting that anti-cancer drugs provide neuroprotective effects in multiple models associated with AD and PD (Cramer et al., 2012; Tanabe et al., 2014). For example, sorafenib, a drug approved for the treatment of primary kidney cancer protects primary cortical neurons against toxicity caused by leucine-rich repeat kinase-2 (LRRK2) (Lee et al., 2010), the mutation of which is a common cause of PD. Nilotinib, which is for treating chronic myelogenous leukemia, protects dopaminergic neurons and improves motor behavior through degrading α-synuclein in various PD animal models (Hebron et al., 2013; Karuppagounder et al., 2014; Mahul-Mellier et al., 2014). These studies indicate that some anti-cancer drugs may have the potential to be developed for the treatment of brain disorders.

We have previously demonstrated that SU4312 (3-[4-(dimethylamino)benzylidenyl]indolin-2-one), initially designed as a candidate drug for cancer therapy due to its inhibition on vascular endothelial growth factor (VEGF) receptor-2 tyrosine kinase, unexpectedly protects against MPP^+-induced neurotoxicity in cells and zebrafish (Cui et al., 2013). However, the detailed mechanisms underlying such neuroprotection have not been fully elucidated, and the effects of SU4312 on rodent models associated with PD have not been characterized. In this current study, we extend our efforts to further explore the novel molecular mechanisms by which SU4312 confers its neuroprotections in both dopaminergic cells and mice models.

2. Materials and methods

2.1. Materials

SU4312 (Purity≥98%), MPTP and MPP^+ were purchased from Sigma (St Louis, MO, USA). Antibody against tyrosine hydroxylase (TH) was from Millipore (Beverly, MA, USA). Antibodies against phospho-Akt (Ser473), total Akt, phospho-GSK3β (Ser9), total GSK3β, MEF2D, Histone-H3, Bax, Bcl-2, caspase-3, cytochrome *c* and β-actin were from Cell Signaling Technology (Beverly, MA, USA). Antibodies against PGC-1α, Tfam and HO-1 were from Santa Cruz Biotechnology (Santa Cruz, CA, USA). Dulbecco's modified

Eagle's medium (DMEM), horse serum (HS), fetal bovine serum (FBS), penicillin and streptomycin were from Invitrogen (Carlsbad, CA, USA).

2.2. Cell culture

PC12 cells were purchased from the American Type Culture Collection (Manassas, VA, USA). Cells were grown in DMEM supplemented with 10% HS, 5% FBS and 1% penicillin/streptomycin mixture at 37 °C under an atmosphere of 5% CO_2 and 95% air.

2.3. MTT assay

MTT assay for measuring cell viability was performed as we previously described (Hu et al., 2015a). Briefly, PC12 cells were pre-treated with 10 μM SU4312 for 2 h, then exposed to 2.5 mM MPP^+. 48 h after treatment, cells were incubated with MTT solution for 4 h. The generated formazan crystal was dissolved in DMSO and the absorbance was examined at a test wavelength of 570 nm with 655 nm as a reference wavelength.

2.4. Hoechst staining

Hoechst staining for evaluating the apoptotic nuclei was carried out as we previously reported (Hu et al., 2015b). Briefly, after treatment, cells were incubated with Hoechst 33,342 (5 μg/ml) for 5 min and visualized using a fluorescence microscope. Cells with bright blue fragmented nuclei showing condensation of chromatin were taken as apoptotic cells.

2.5. MEF2 luciferase reporter gene assay

MEF2 luciferase reporter assay was performed as we previously described (Hu et al., 2015b). Briefly, PC12 cells were transfected with a MEF2:pGreenFire1™ reporter lentivector (System Biosciences, Mountain View, CA, USA). 48 h after transfection, cells were treated with SU4312 for another 48 h, or pre-treated with SU4312 for 2 h prior to a 48-h insult of MPP^+, and then cellular extracts were assayed for luciferase activities.

2.6. ShRNA assay

The short hairpin RNA (shRNA) against MEF2D assay was performed as we previously reported (Hu et al., 2015b). Briefly, PC12 cells were transfected with the indicated plasmids by using Lipofectamine 2000 at the ratio of 1:2 (plasmids: liposome). Selection media that contained 100 μg/ml G418 (Sigma Chemicals, St Louis, MO, USA) were added to the cells 24 h after transfection. Experiments were carried out 48 h after the cells were transfected.

2.7. Animals and treatment

All experimental procedures were conducted according to the guidelines of Jinan University Ethic Committee for the Care and Use of Laboratory Animals (Approval No. SCXK2013-0034). Male C57BL/6 mice (23 ± 2 g body weight, 10 weeks of age) were supplied by Guangdong Medical Laboratory Animal Center. Mice were maintained in a room with 12-h light/dark cycles at 20–25 °C and relative humidity of 60%, and received food and water *ad libitum*. Five groups of mice (n = 8/group) were assigned for this study. To induce an acute experimental Parkinsonism, the mice were injected *i.p.* with 20 mg/kg MPTP hydrochloride, at 2-h intervals for a total of four injections in one day. On the next three days, SU4312 (0.2 and 1 mg/kg) and rasagiline (0.1 mg/kg) were administrated *i.g.* once a day.

2.8. Behavioral test

2.8.1. Rotarod test

One day before testing, mice were trained until they could remain on a rotarod (Zhenghua Biologic Apparatus Facilities, China) for 120 s without falling. During the test, mice were placed on the rotary apparatus which started at 5 rpm for 30 s and then accelerated to 40 rpm within 5 min. Each trial would end when the mouse fell off from the rotarod, and the latency (time) was recorded. Each animal was tested in three independent trials, each with 1 h of intertribal interval.

2.8.2. Gait test

Mice were subjected to training trials to acclimatize to the environment. During the test, mice were placed in a 5 cm wide, 5 cm high and 85 cm long corridor, whose floor was covered with white absorbing paper. The handpaws of mice were colored with black inks. The total footsteps were recorded on the white absorbing paper. Average stride length was calculated as the distance between successive paw footprints. Meanwhile, the time that it took the mice to go through the corridor was also recorded. Each animal was tested in three independent trials, each with 1 h of intertribal interval.

2.9. Immunohistochemistry

For the study of tyrosine hydroxylase (TH) staining, 24 h after the administration of the last dose of SU4312 or rasagiline, four mice in each group were randomly chosen and sacrificed. Brain-tissue processing and immunohistochemistry were carried out as we previously described (Guo et al., 2016). Briefly, mice brains were fixed with 4% PFA after transcardiac perfusion, paraffinembedded, and cut into 5 μm coronal sections encompassing the entire SNpc. TH-positive cells were counted by observers blind to the experimental protocol on a stereomicroscope (BX51, Olympus Corp., Tokyo, Japan) using the optical fractionator method as described previously (Finkelstein et al., 2004; Mandir et al., 1999).

For dual-labeled immunofluorescence, after an antigen retrieval procedure, brain sections were incubated with 1% TritonX-100 for 30 min and blocked with 10% horse serum in PBS (0.01 M, pH 7.4) for 2 h at room temperature. Thereafter, sections were incubated overnight at 4 °C with primary antibodies against 8-OHdG (1:100 dilutions), 4-HNE (1:100 dilutions) and 3-NT (1:100 dilution). After washing twice, the sections were incubated with biotin-conjugated universal secondary antibody for 2 h, and visualized using a fluorescence microscope (OLYMPUSCKX41, Tokyo, Japan).

2.10. Electrochemical HPLC determination of striatal dopamine and its metabolites, 3,4-dihydroxyphenylacetic acid (DOPAC) and homovanilic acid (HVA)

The remaining 4 mice in each group were anesthetized and sacrificed. The extracted striatum was homogenized in 0.1 N perchloric acid (v/w = 10:1), and the homogenate was centrifuged at 12,000 g for 20 min at 4 °C. The supernatant was then collected and detected by the HPLC-ED system equipped with an Agilent Eclipse Plus C18 reverse phase column (4.6 × 150 mm). The mobile phase had the following composition: 50 mM NaH_2PO4, 0.03 mM EDTA, 0.8 mM sodium octyl sulfate, 30 ml/L methanol (pH 3.5) and used at a flow rate of 1 ml/min. The potential was 0.52 V to determine dopamine peak by electrochemical detection. The dopamine levels in the samples were quantified by extrapolating the peak area from a standard curve constructed under the same conditions. Mouse brain levels of dopamine and its main metabolites were expressed as ng/mg tissue weight.

2.11. MAO-B inhibition assay in vitro and in vivo

The MAO-B inhibition activity of SU4312 was determined according to the instructions supplied in the MAO-Glo™ assay kit. Briefly, SU4312 was incubated in 96-well opaque white plates with MAO substrate and rhMAO-B (final concentration: 0.25 mg protein/ml) for 1 h at room temperature. This reaction was then terminated by adding a stop solution, and luminescence was determined using a luminometer. Selegiline, a known MAO-B inhibitor, served as a positive control. For the determination of IC_{50} values, the MAO-B inhibition assay was carried out using a fixed concentration of substrate and varying concentrations of SU4312.

For *in vivo* MAO-B inhibition activity, SU4312 (0.2, 1 mg/kg) and selegiline (10 mg/kg) were administrated *i.g* to male C57BL/6 mice (n = 6/group). Mice were sacrificed 24 h after drug administration, and the tissue homogenates of cerebellum, liver and intestine were prepared as we previously described (Guo et al., 2016). MAO-B activity of homogenates was determined as aforementioned. The percentage of MAO-B inhibition was calculated as follows: $(A_{vehicle} - A_{drug})/A_{vehicle} \times 100\%$, where $A_{vehicle}$ and A_{drug} are the MAO-B activity of vehicle-treated sample and drug-treated sample, respectively.

2.12. Molecular docking

Molecular docking analysis was performed using Molecular Operating Environment (MOE, version 2016.08, Chemical Computing Group Inc., Montreal, QC, Canada). The molecular model of MAO-B was built from the X-ray co-crystal structure of the human MAO-B in complex with the selective inhibitor safinamide (PDB: 2V5Z). Hydrogen and missing heavy atoms were added to the receptor structure, and atom types and partial charges were assigned. The model was then subjected to local energy minimization to identify the optimal position by using the conjugate gradient algorithm and analytical derivatives in the internal coordinates. Docking experiments were carried out using the default parameters of MOE (Placement: Triabgle Matcher, Rescoring 1: London dG, Refinement: Rigid Receptor, Rescoring 2: GBV1/WSA dG).

2.13. Western blotting

Western blot analysis was performed as we previously described (Hu et al., 2015a). After treatment, cells or brain tissues were lysed in lysis buffer on ice. Protein was then extracted and collected by centrifugation, separated on SDS–polyacrylamide gel, and finally transferred onto polyvinyldifluoride membranes. After 2 h of blocking at room temperature, the membranes were probed with various primary antibodies (1:1000 for PGC-1α, Tfam, HO-1, phospho-Ser-473-Akt, total Akt, phospho-Ser-9-GSK3β, total GSK3β, Bax, Bcl-2, caspase-3, cytochrome *c*, MEF2D and TH; 1:2000 for Histone-H3 and β-actin) overnight at 4 °C, followed by 45 min of incubation with secondary antibodies (1:2000). The blots were developed using an enhanced chemiluminescence plus kit (Amersham Bioscience, Aylesbury, UK), exposed to autoradiographic films, and quantified by densitometric analysis.

2.14. Statistical analysis

Data were expressed as mean ± SD. Data analyses were performed with the GraphPad Prism software (GraphPad, San Diego, CA, USA). Multiple comparisons were made using one-way ANOVA, followed by the Tukey's *post hoc* test. $P < 0.05$ was considered to be statistically significant.

3. Results

3.1. SU4312 effectively protects against mitochondria-dependent apoptotic pathway in PC12 cells caused by MPP^+

We had previously demonstrated that SU4312 effectively promoted PC12 cell viability from MPP^+-induced insult using MTT assay (Cui et al., 2013). It was evident that SU4312 dose-dependently prevented the neurotoxicity caused by MPP^+, with a maximum effect at 10 μM (Cui et al., 2013). Therefore, we chose SU4312 at 10 μM for all the subsequent cellular experiments in the present study. To further analyze whether the neuroprotection of SU4312 was achieved through an anti-apoptotic manner, Hoechst staining was used in our model. It was found that pre-treatment with SU4312 for 2 h markedly decreased the number of condensed nuclei stained by Hoechst (Fig. 1A and B) caused by MPP^+. Since MPP^+-induced apoptosis contributes to PC12 cell death by activating the mitochondrial caspase pathway, immunoreactivity of Bax, Bcl-2, caspase-3 and cytosolic cytochrome *c* was examined. It was evident in Fig. 1C that SU4312 significantly reversed the increase in protein expression of Bax/Bcl-2, caspase-3, and cytosolic cytochrome *c* caused by MPP^+.

3.2. SU4312 enhances MEF2 gene transactivation activity under basal and pathological conditions

It has been reported that activation of MEF2 contributes to neuronal survival in several experimental paradigms (She et al., 2011; Wang et al., 2009). We then tested the possibility that SU4312 may enhance MEF2 transcriptional activity. We transfected PC12 cells with MEF2-dependent luciferase reporter construct and treated these cells with SU4312 for 48 h (basal condition), or pre-treated these cells with SU4312 2 h prior to the 48-h MPP^+ exposure (pathological condition). This analysis clearly indicated that SU4312 stimulated MEF2 transcriptional activity under both basal and pathological conditions (Fig. 2).

3.3. SU4312 confers neuroprotection through the activation of MEF2D in PC12 cells

To judge whether the activation of transcription factor MEF2, and MEF2D in particular, contributes to the neuroprotection of SU4312, we evaluated the protein expression of MEF2D in nucleus using Western blotting. It was evident that SU4312 greatly reversed the inhibition of nuclei MEF2D caused by MPP^+ (Fig. 3A). Moreover, with the use of ShRNA technique, genetic depletion of MEF2D significantly abolished the neuroprotection of SU4312 against MPP^+ in PC12 cells (Fig. 3B).

3.4. SU4312 reverses the inhibition of PI3K/Akt/GSK3β pathway caused by MPP^+ in PC12 cells

It has been well documented that MEF2 activity could be negatively regulated by GSK3β (Rashid et al., 2014). We examined whether SU4312 could potentiate PI3-K/Akt to down-regulate the MEF2 inhibitor GSK3β. First, LiCl, the specific inhibitor of GSK3β, promoted neuronal survival in our model (Fig. 4A), which is indicative of the involvement of GSK3β in the neurotoxicity of MPP^+. Second, LY294002, the specific PI3-K inhibitor, significantly abolished SU4312-mediated neuroprotection against MPP^+ (Fig. 4A). Furthermore, a rapid decrease in protein expression of *p*-

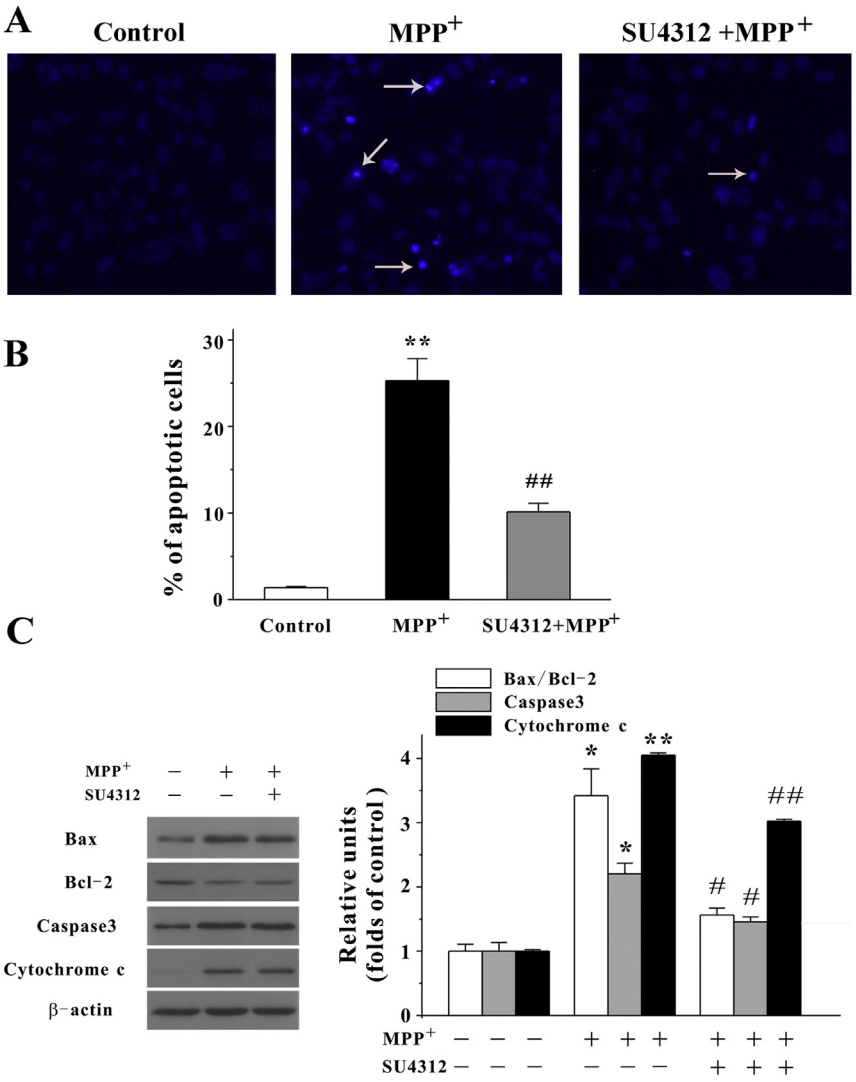

Fig. 1. SU4312 prevents mitochondria-dependent apoptosis in PC12 cells caused by MPP$^+$. PC12 cells were pre-treated with 10 μM SU4312 for 2 h, then exposed to 2.5 mM MPP$^+$. 48 h after treatment, cells were incubated with Hoechst 333258 (5 μg/ml) for 10 min, and then observed using a fluorescence microscope (A). The apoptotic cells that displayed a condensed bright blue chromatin in (A) were quantitatively measured (B). The sister PC12 cells treated as above were lysed and subjected to Western blot assay using specific antibodies against Bax, Bcl-2, caspase-3 and cytochrome *c* (C). *, $p < 0.05$, **, $p < 0.01$, compared to control group; #, $p < 0.05$, ##, $p < 0.01$ compared to MPP$^+$ group.

Ser473-Akt and *p*-Ser9-GSK3β was observed in PC12 cells after exposure to MPP$^+$. Pre-treatment with SU4312 for 2 h greatly reversed these changes (Fig. 4B). Similarly, LY294002 significantly abrogated the up-regulated protein levels of *p*-Ser473-Akt and *p*-Ser9-GSK3β induced by SU4312 (Fig. 4B).

3.5. SU4312 alleviates dysfunction in motor behavior in mice insulted with MPTP

After confirming the neuroprotective effects of SU4312 *in vitro*, SU4312 was intragastrically administered to MPTP-insulted PD model of C57BL/6 mice, and the mice were evaluated behaviorally using rotarod and gait tests. As demonstrated in Fig. 5, MPTP significantly decreased the latency to fall from the rotarod, but the decrement of latency was significantly lower in the SU4312-treated mice than in the MPTP-treated mice (Fig. 5A). Furthermore, when gait test was performed, results demonstrated that MPTP shortened the stride length (Fig. 5B) as well as the time to get across the corridor (Fig. 5C), both of which were dose-dependently reversed by SU4312.

3.6. SU4312 rescues DA neurons from MPTP insult and attenuates decrease in dopamine as well as its metabolites level in mice

As clearly demonstrated in Fig. 6A, TH immunostaining analysis revealed that MPTP caused an approximately 30% loss in TH-positive neurons in mice, which was remarkably inhibited by SU4312 (0.2 and 1 mg/kg) and rasagiline (0.1 mg/kg) Similarly, results of Western blotting assay indicated that SU4312 effectively reversed the decrease in protein expression of TH caused by MPTP (Fig. 6B). Consistent with the changes in DA neurons, the levels of striatal dopamine and its metabolites DOPAC and HVA all decreased greatly after the MPTP insult, as assayed by electrochemical HPLC. SU4312 (0.2 and 1 mg/kg) partially inhibited these changes (Fig. 7). Particularly, SU4312 and rasagiline had comparable efficacy in reversing the inhibition of DOPAC and HVA caused by MPTP.

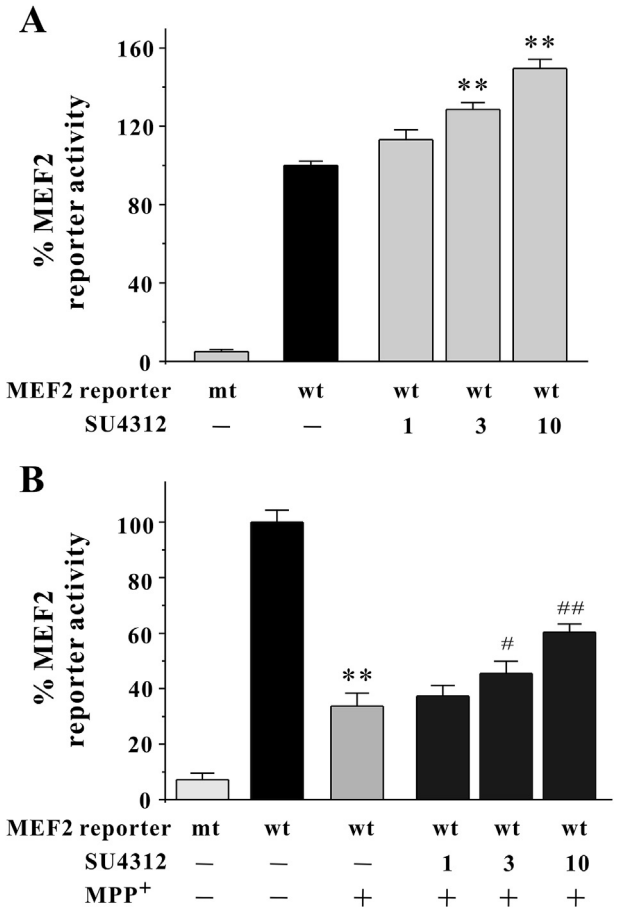

Fig. 2. SU4312 enhances MEF2 gene transactivation activity under basal and pathological conditions. (A) PC12 cells were transfected with MEF2 luciferase reporter construct and treated with or without SU4312 (1–10 μM). 48 h after treatment, cells were subjected to luciferase reporter assay. (B) PC12 cells transfected with MEF2 luciferase reporter construct were pre-treated with SU4312 for 2 h, and then exposed to 2.5 mM MPP^+. 48 h after treatment, the luciferase reporter activity was measured. **, $p < 0.01$, compared to control group; #, $p < 0.05$ and ##, $p < 0.01$, compared to MPP^+ group.

3.7. SU4312 inhibits the formation of 8-OHdG, 4-hydroxynonenal (4-HNE) and 3-nitrotyrosine (3-NT) in the substantia nigra of MPTP-treated mice

8-OHdG (a product of DNA oxidation), 4-HNE (a product of lipid peroxidation), and 3-NT (a product of protein nitrosylation) are widely used as biomarkers of oxidative damage. Immunofluorescence analysis of the MPTP-treated substantial nigra section showed a dramatic increase in 8-OHdG and 4-HNE formation in the DA neurons (Fig. 8), as evidenced by the TH and 8-OHdG double immunolabeling, while SU4312 significantly abolished MPTP-induced generation of 8-OHdG and 4-HNE in DA neurons. Similarly, there was a sharp increase in the expression of 3-NT in sections from the MPTP-treated mice, which was dose-dependently inhibited by SU4312 treatment (Fig. 9).

3.8. SU4312 activates MEF2D via activation of PI3-K/Akt/GSK3β signaling pathway in the SNpc of mice insulted by MPTP

To confirm the molecular mechanisms observed in PC12 cells, *in vivo* assessment of PI3-K/Akt/GSK3β pathway was performed. As seen in Fig. 10, MPTP caused a significant decrease in protein levels of MEF2D, *p*-Ser473-Akt and *p*-Ser9-GSK3β, which were substantially inhibited by SU4312 (0.2 and 1 mg/kg). Notably, the levels of MEF2D and *p*-Ser473-Akt in SU4312 group returned to those in the control group.

3.9. SU4312 increases the expression of mitochondrial biogenesis-related proteins in the SNpc of mice insulted by MPTP

It has been reported that mitochondrial biogenesis could modulate mitochondrial function and promote neuronal recovery from damage caused by neurotoxins. We further tested the possibility that SU4312 may induce mitochondrial biogenesis in mice insulted with MPTP. It was found that SU4312 dose-dependently reversed MPTP-inhibited protein expression of peroxisome proliferator-activated receptor gamma co-activator (PGC-1α), mitochondrial transcription factor A (TFAM) and heme oxygenase-1 (HO-1) (Fig. 11).

3.10. SU4312 inhibits MAO-B activity both in vitro and in vivo

Prior to evaluating the inhibitory effects of SU4312 on MAO-B, we first investigated its effects on MAO-A in cultured PC12 cell line, since these cells contain only MAO-A (Weinreb et al., 2006). It was found that SU4312 did not show any significant inhibitory effects on MAO-A activity, even when the concentration exceeded 100 μM, SU4312 only mildly inhibited MAO-A (data not shown). Then, the inhibitory effects of SU4312 on MAO-B were investigated *in vitro*, *in vivo* and by computational simulation, respectively. A dose-response curve was plotted after incubation with SU4312 and MAO substrate for 1 h and it was found that SU4312 dramatically inhibited MAO-B activity *in vitro* with an IC_{50} value of 0.2 μM (Fig. 12A). Furthermore, administration of SU4312 (1 mg/kg, *i.g.*) greatly inhibited MAO-B activity in the mouse brain and intestine, but not in the liver (Fig. 12B). Selegiline (10 mg/kg, *i.g.*) substantially attenuated the activity of MAO-B in all three tissues, setting as a positive control. Furthermore, molecular docking via MOE-Dock program demonstrated the lowest energy pose with a binding free energy of SU4312 for MAO-B (PDB: 2V5Z) was −7.6 kcal/mol. This analysis also revealed that SU4312 occupied the MAO-B activate site (Fig. 12C up-panel), the entrance cavity close to residue Ser59, similar to the known MAO-B inhibitor safinamide (binding energy for MAO-B: −6.2 kcal/mol). It was noted that the *N, N*-dimethyl moiety of SU4312 formed hydrogen bond to Cys172 in MAO-B (Fig. 12C down-panel).

4. Discussion

PD is a complicated neurodegenerative disorder with multifactorial pathologies, including mitochondrial dysfunction, autophagy, oxidative stress, progressive loss of DA neurons in SNpc and increased MAO enzyme activity (Trinh and Farrer, 2013). Therefore, it is necessary to identify multifunctional agents that can affect more than one target involved in the disease pathology. In the present study, we provide direct evidence that the anti-cancer agent SU4312 substantially protected against MPP^+-induced neurotoxicity in neuronal cell lines and in MPTP mice via the activation of MEF2D. Moreover, SU4312 selectively inhibited the activity of MAO-B *in vitro* and *in vivo*. Our data strong suggest that SU4312 could be a potential candidate for further preclinical study aimed at the prevention and treatment of PD.

Since survival factor MEF2D could be regulated by a variety of factors, including the aforementioned processes, therapy that targets MEF2D represents an attractive therapeutic strategy. Indeed, there is evidence suggesting that activation of MEF2D *in vivo* rescues SNpc DA neurons from neurotoxicity in PD animal models (Smith et al., 2006). Very discouragingly, the use of recombinant

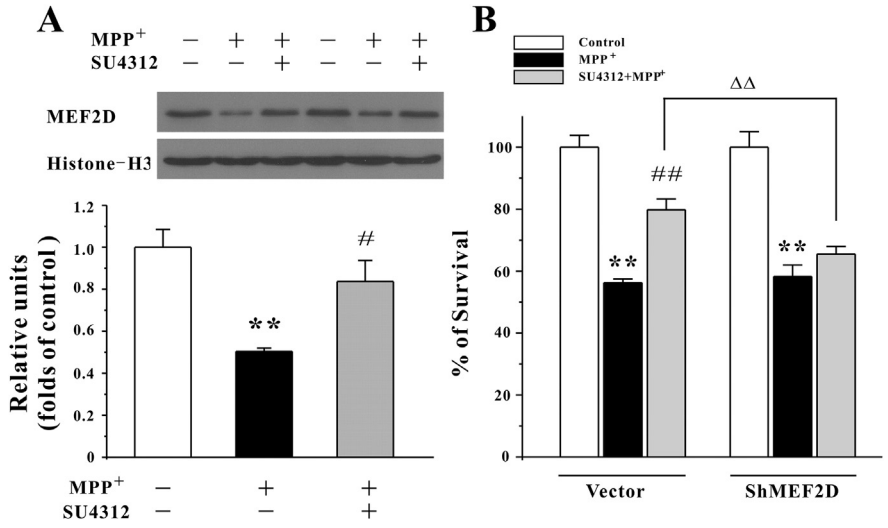

Fig. 3. Activation of MEF2D contributes significantly to the neuroprotection of SU4312. (A) SU4312 alleviated MPP^+-induced inhibition of MEF2D expression in nuclear compartments in PC12 cells. Cells were pre-treated with or without 10 μM SU4312 for 2 h, then exposed to 2.5 mM MPP^+. 48 h after treatment, lysates from nuclear extracts were subjected to Western blot assay using antibodies against MEF2D or Histone-H3 (nuclear loading control). (B) Genetic depletion of MEF2D using ShRNA significantly abrogated SU4312-mediated neuroprotection. PC12 cells were transfected with pGPU6-green fluorescent protein plasmid (Vector) and pGPU6 plasmid encoding MEF2D ShRNA (ShMEF2D). After transfection, cells were treated as in (A), and subjected to MTT assay for measuring cell viability. **, $p < 0.01$, compared to control group; #, $p < 0.05$, ##, $p < 0.01$, compared to MPP^+ group; $^{\triangle\triangle}$, $p < 0.01$, SU4312 plus MPP^+ groups between Vector and ShMEF2D.

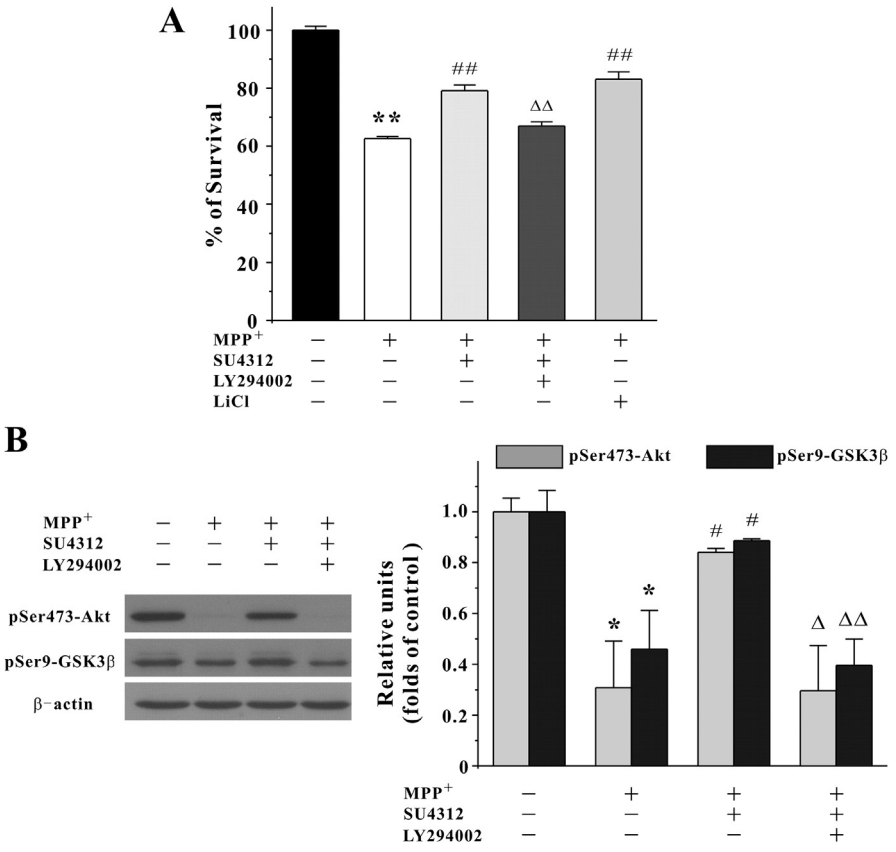

Fig. 4. SU4312 reverses the inhibition of PI3K/Akt/GSK3β pathway caused by MPP^+. PC12 cells were pre-treated with PI3K inhibitor LY294002 (10 and 30 μM) for 2 h, then incubated with SU4312 for 2 h, and finally exposed to 2.5 mM MPP^+ for 48 h. Cells were subjected to MTT assay for measuring viability (A), or Western blot assay for investigating the protein expression of pSer473-Akt, t-Akt, pSer9-GSK3β and t-GSK3β (B). *, $p < 0.05$, **, $p < 0.01$, compared to control group; #, $p < 0.05$, ##, $p < 0.01$, compared to MPP^+ group; $^{\triangle}$, $p < 0.05$, $^{\triangle\triangle}$, $p < 0.01$, compared to SU4312 plus MPP^+ group.

viral approach to stimulate MEF2D transcriptional activity in these studies severely limits their further practical application. Here, we identified a small molecule SU4312 as a potent activator of MEF2D, a conclusion supported by the fact that SU4312 enhanced MEF2D

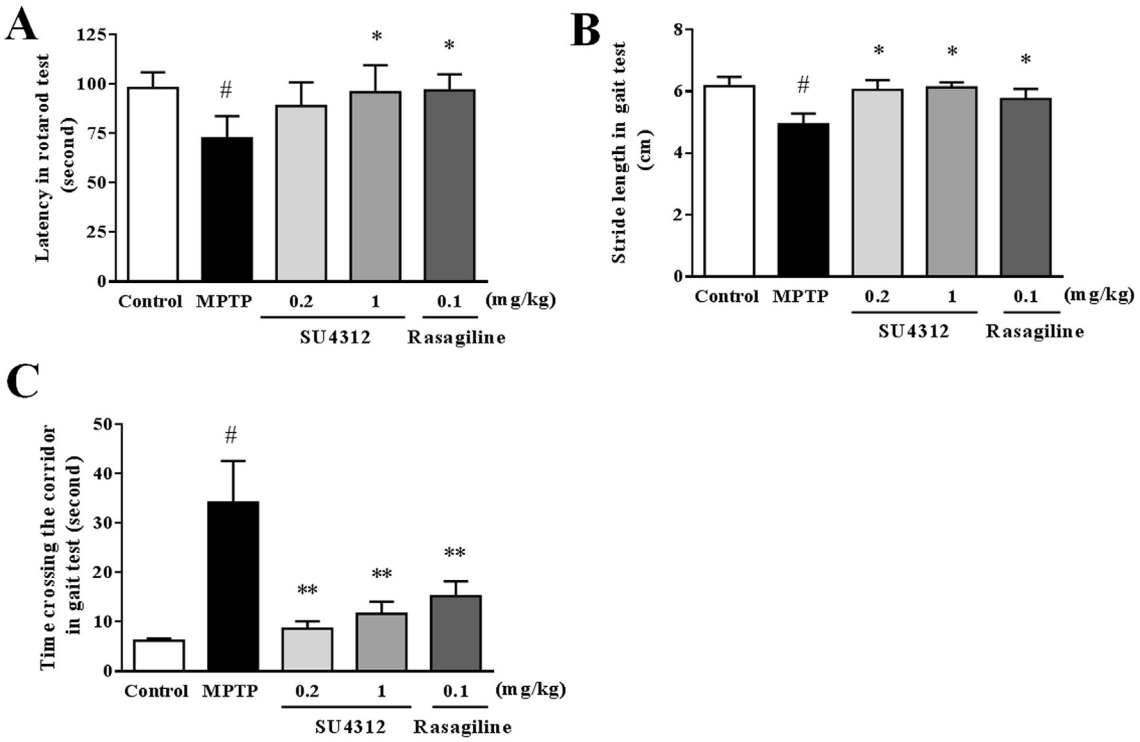

Fig. 5. SU4312 alleviates motor deficits in mice insulted by MPTP. (A) The latency of mice to fall down from the rotarod. (B) The stride length of mice in gait test. (C) The time of mice to cross the corridor in gait test. #, $p < 0.05$, compared to control group; *, $p < 0.05$ and **, $p < 0.01$, compared to MPTP group.

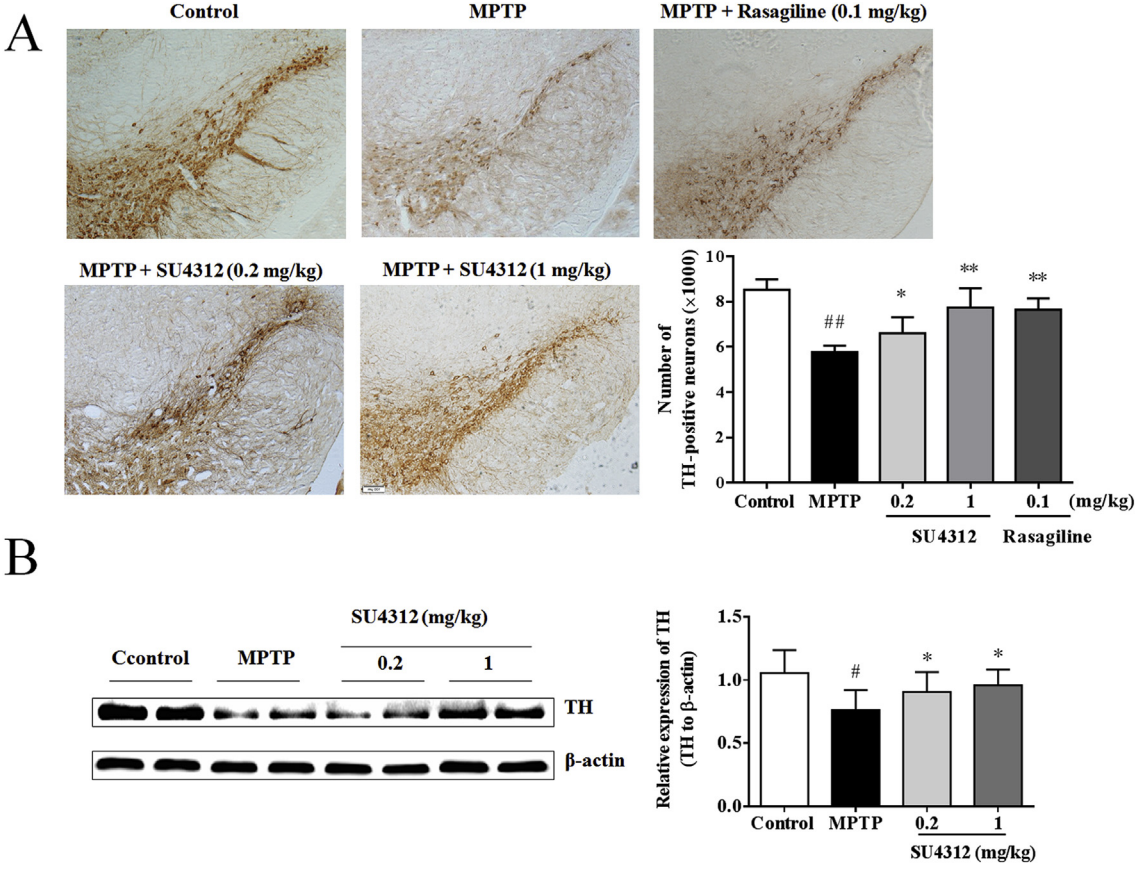

Fig. 6. SU4312 increased the number of TH-positive neurons and TH expression in the SNpc of mice insulted by MPTP. Midbrain slices were prepared and subjected to immunohistochemistry for quantification of TH-positive neurons (A), or to Western blotting assay for measurement of protein expression of TH. #, $p < 0.05$ and ##, $p < 0.01$, compared to control group; *, $p < 0.05$ and **, $p < 0.01$, compared to MPTP-treated group.

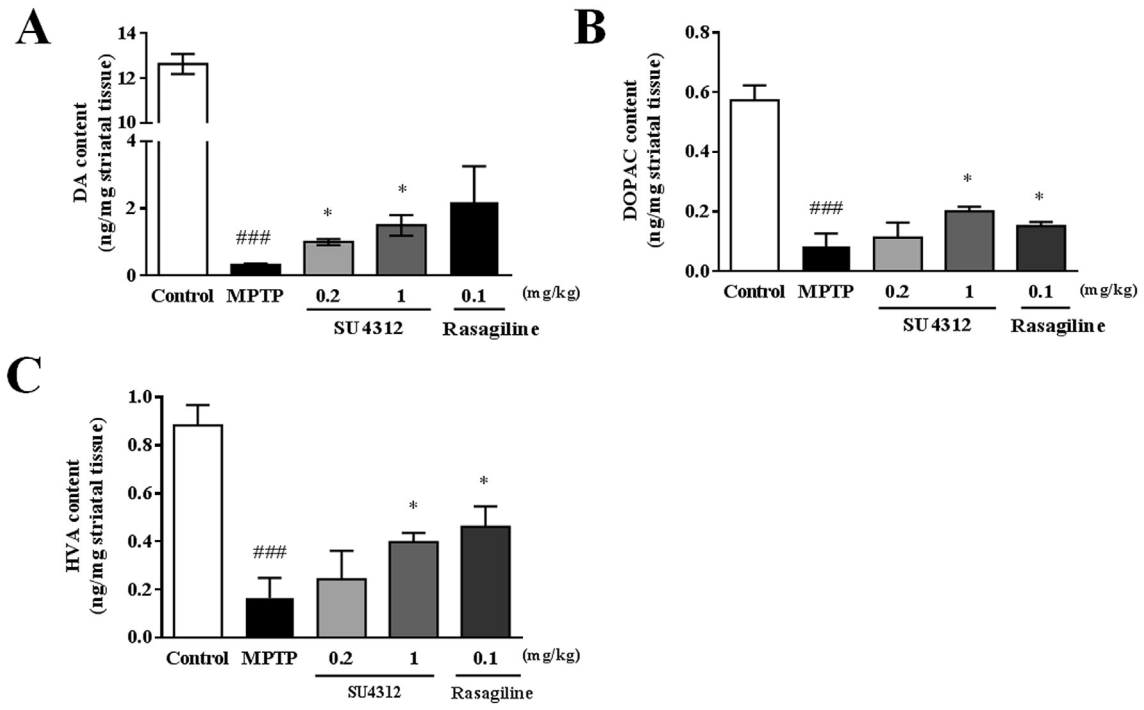

Fig. 7. SU4312 reverses the reduction of DA and it metabolites in the striatum of mice insulted by MPTP. The levels of striatal dopamine (A) and its metabolites DOPAC (B) and HVA (C) were analyzed using electrochemical HPLC. ###, $p < 0.001$, compared to control group; *, $p < 0.05$, compared to MPTP group.

transcriptional activity under both basal and pathological conditions. Moreover, we found that the neuroprotection of SU4312 as observed in cellular and animal studies was achieved mainly through the activation of MEF2D, as gene depletion of MEF2D rendered SU4312 largely ineffective in protecting neuronal cell lines from MPP^+ insult. Besides, our findings that SU4312 markedly attenuated the immunoreactivity of biomarkers of oxidation and nitrogen free radical species in mice brain sections indicate that the anti-oxidative activity of SU4312 may also account for its neuroprotection. Lastly, the present results demonstrated that SU4312 effectively inhibited the mitochondria-dependent apoptotic pathway by blocking the release of cytochrome *c* from mitochondria, and that SU4312 promoted mitochondrial biogenesis by up-regulating PGC-1α/TFAM/HO-1, suggesting that the attenuation of mitochondrial dysfunction is another important mechanism underlying the neuroprotection of SU4312. Most encouragingly, our previous work has shown that SU4312 could be well absorbed and could readily cross the blood-brain barrier (Cui

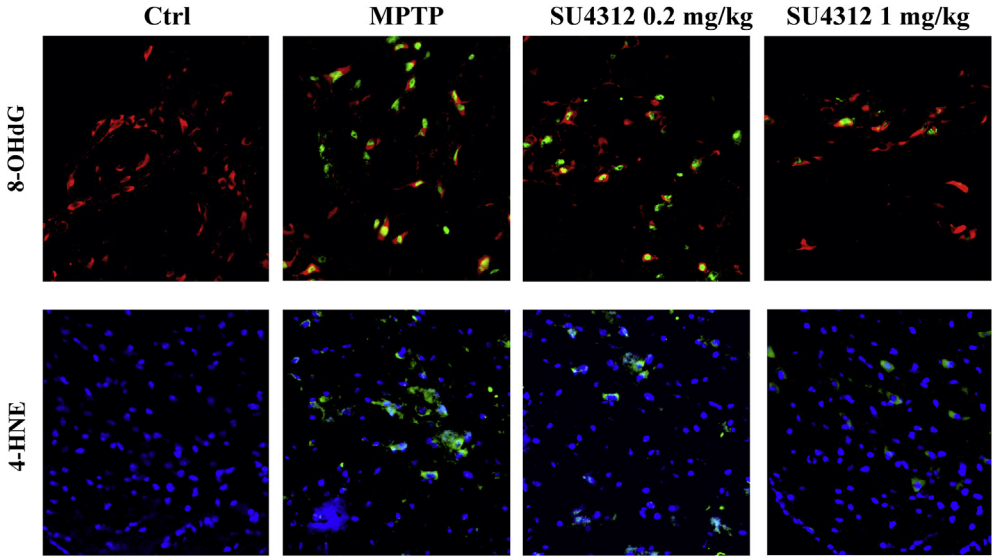

Fig. 8. SU4312 inhibits the formation of 8-OHdG and 4-HNE in the substantial nigra of MPTP-treated mice. (A) Representative images of 8-OHdG immunostaining showed that SU4312 prevented the oxidative DNA damage. 8-OHdG (green) co-localized with TH (red)-positive DA neurons. (B) Representative images of 4-HNE (green) immunostaining demonstrated that SU4312 blocked lipid peroxidation. Nuclei were counterstained with DAPI (blue). (For interpretation of the references to colour in this figure legend, the reader is referred to the web version of this article.)

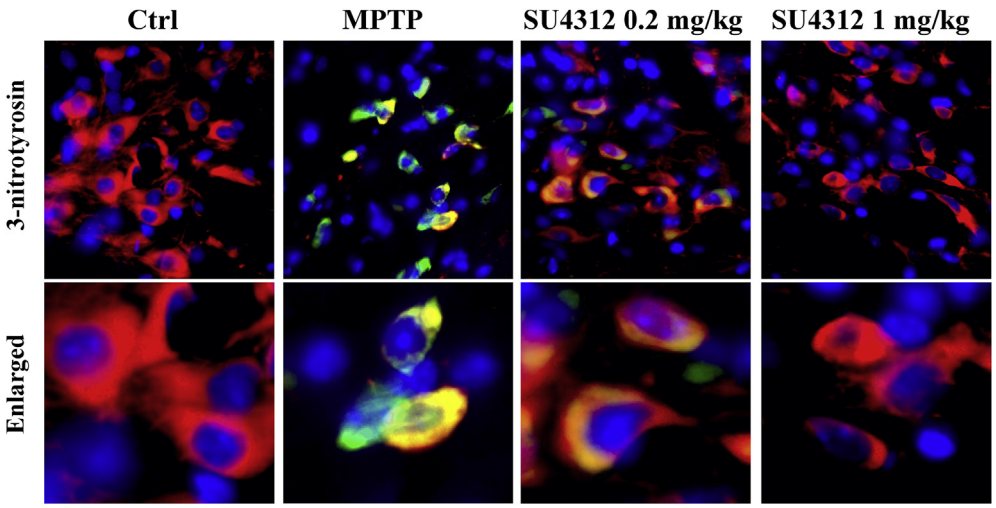

Fig. 9. SU4312 inhibits the formation of 3-NT in the substantial nigra of MPTP-treated mice. 3-NT (green) co-localized with TH (red)-positive neurons. Nuclei were counterstained with DAPI (blue). (For interpretation of the references to colour in this figure legend, the reader is referred to the web version of this article.)

et al., 2013), strongly suggesting that SU4312 could be developed as drugs for brain disorders. And notably, SU5416 and sunitinib, the analogs of SU4312 with 3-substituted-2-indolin pharmacophore, both displayed stimulatory effects on MEF2 in PC12 cells (preliminary data). It would be highly interesting to test these analogs in more PD models to validate their therapeutic potential fully.

The regulation of MEF2 activity is complicated. A number of survival and death-related signals exhibit their stimulatory or inhibitory effects on MEF2 (Wang et al., 2009). The phosphorylation in the transactivation domain by extracellular signal regulated kinase5 (ERK5) (on MEF2A, 2C, and 2D), p38 kinase (on MEF2A and 2C) or Protein kinase A (on MEF2C) increases the transcriptional activity of MEF2, which in turn enhances neuronal survival (Rashid et al., 2014; Wang et al., 2009). In contrast, both GSK3β (on MEF2D) and CDK5 (on MEF2A, 2C, and 2D)-mediated phosphorylation decline MEF2-dependent transcription and inhibit MEF2 function in response to overt neurotoxic insults (Rashid et al., 2014). Taking GSK3β as an example, neurotoxins (MPP^+, 6-OHDA) or neuronal activity deprivation activated GSK3β in the nucleus, resulting in GSK3β-dependent inhibition of MEF2D function, whereas overexpression of MEF2D mutant, which is resistant to GSK3β inhibition, protected neurons from such neurotoxicity (Wang et al., 2009). These findings identify survival factor MEF2D as a novel downstream effector targeted by GSK3β. Our current investigation revealed that SU4312 indirectly inhibited GSK3β *in vitro* and *in vivo* in a PI3-K/Akt-dependent manner, suggesting SU4312-induced MEF2D activation may, at least partially, result from its inhibitory effects on GSK3β. Additionally, recent studies have highlighted linkage between neuronal nitric oxide synthase (NOS)/Nitric oxide (NO) system and MEF2 (Okamoto et al., 2014; Pon and Marra, 2016). It is reasonable to assume that the anti-neuronal NOS activity of SU4312, which has been demonstrated in our previous study (Cui

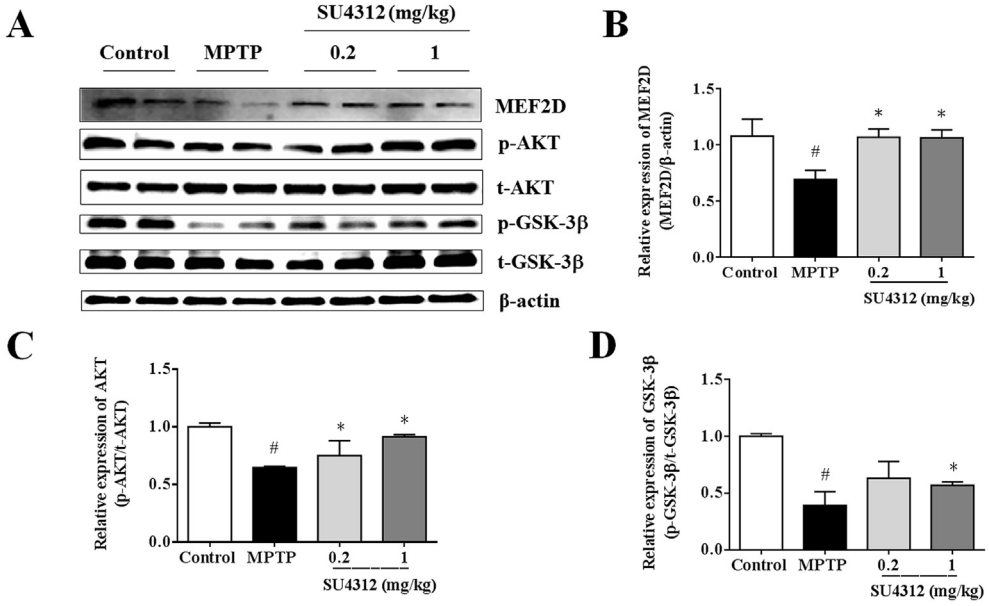

Fig. 10. SU4312 activates MEF2D via activation of PI3-K/Akt/GSK3β in the SNpc mice insulted by MPTP. The brain tissues were lysed and subjected to Western blot ting assay using antibodies against MEF2D, pSer473-Akt, t-Akt, pSer9-GSK3β and t-GSK3β. #, $p < 0.05$, compared to control group; *, $p < 0.05$, compared to MPTP group.

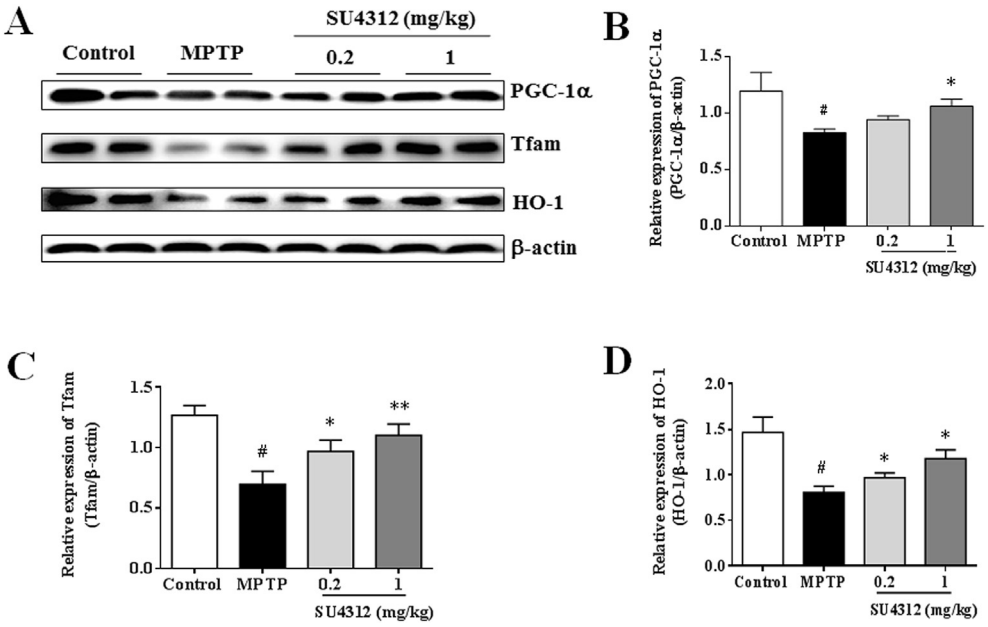

Fig. 11. SU4312 increases the expression of mitochondrial biogenesis-related proteins in the SNpc of mice insulted by MPTP. The brain tissues were lysed and subjected to Western blot ting assay using antibodies against PGC-1α, Tfam and HO-1. #, $p < 0.05$ compared to control group; *, $p < 0.05$ and **, $p < 0.01$, compared to MPTP-treated group.

et al., 2013), may underlie the activation of MEF2D. However, we could not rule out any other possible contributing targets on the membrane or in the cytoplasm, such as cyclin-dependent kinase 5 (CDK5). A recent study reported that sunitinib potently inhibited CDK5 with an IC_{50} of 4.2 μM (Wrasidlo et al., 2014), suggesting that sunitinib and its analogs (SU4312, SU5416) may activate MEF2 through the inhibition of CDK5. Further investigation will be carried out in our future projects.

MAO-B is an enzyme responsible for dopamine metabolism. MAO-B inhibitors, namely selegiline and rasagiline, block dopamine metabolism and increase the level of dopamine in the brain, thus providing symptoms-relieving benefits for the motor deficiency. In our current study, SU4312 was characterized, for the first time, as a MAO-B inhibitor both *in vitro* and in *vivo*, offering a novel molecular mechanism underlying the potential application of SU4312 for treating PD. Moreover, computational simulation revealed that *N, N*-dimethyl moiety of SU4312 formed hydrogen bond to Cys172 in MAO-B. Since irreversible MAO-B inhibitors such

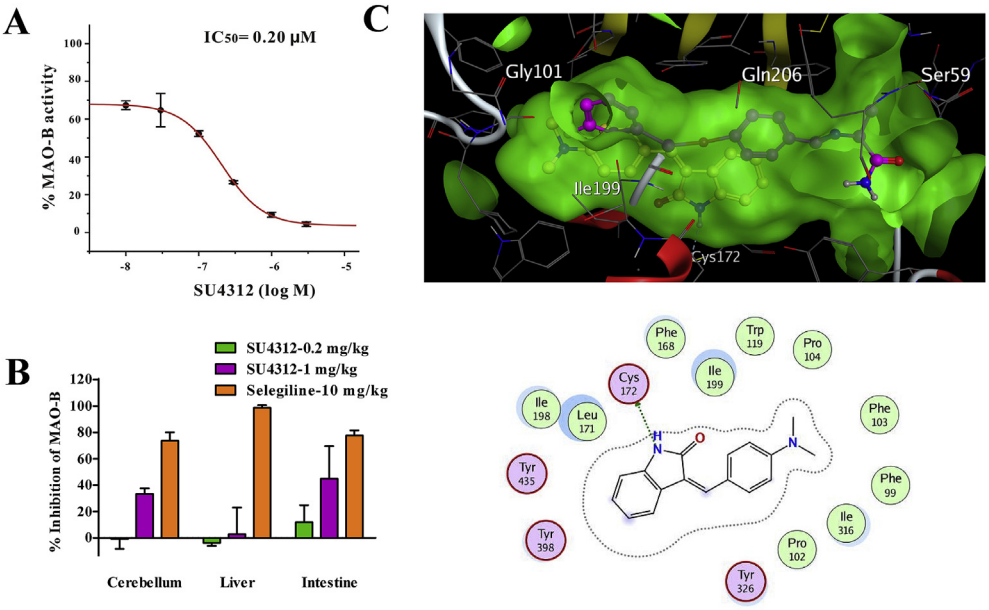

Fig. 12. SU4312 effectively inhibits MAO-B activity both *in vitro* and *in vivo*. (A) SU4312 inhibits MAO-B activity *in vitro*. (B) SU4312 inhibited MAO-B activity *in vivo*. (C) Molecular docking simulation of interaction between SU4312, or a known MAO-B inhibitor safinamide (purple), with MAO-B. (Up panel), Low-energy conformation of SU4312 bound to the pocket of human MAO-B was generated by MOE docking software. SU4312 was depicted as a ball-and-stick model showing carbon (yellow), oxygen (red) and nitrogen (blue). (Low panel), 2D ligand interaction diagram of the docked SU4312 within the binding sites of the MAO-B. (For interpretation of the references to colour in this figure legend, the reader is referred to the web version of this article.)

as rasagiline and selegiline formed a covalent bond with the enzyme's flavin adenine dinucleotide cofactor upon inhibition (Myllyla et al., 1996; Rojas et al., 2015), SU4312 may act as a reversible MAO-B inhibitor. And notably, because PC12 cells contain only MAO type A (Weinreb et al., 2006), it is reasonably to assume that the neuroprotection of SU4312 in PC12 cells was achieved through a MAO-B inhibition-independent manner. Although the inhibitory effects of SU4312 on MAO-B was possibly not related to its neuroprotection on MPTP mice model, as selegiline and rasagiline protected DA neurons independent of their MAO-B inhibition, it is undoubted that MAO-B inhibition of SU4312 would confer amelioration of Parkinsonian motor defects in mice.

In recent years, the research fields offer alternatives to the current paradigm of drug discovery, from the traditional one-drug-one-target model to the new one-drug-multiple-targets approach. Multifunctional compounds may provide greater efficacy than single-target compounds by addressing the various pathological aspects of neurodegenerative diseases. It is well documented that the anticancer activity of SU4312 is achieved through direct inhibition of the proliferation of cancer cells and indirect suppression of angiogenesis (Sun et al., 1998; Tran et al., 2007; Miki et al., 2010). However, we have demonstrated previously that the neuroprotective effects of SU4312 were not directly correlated with its anti-angiogenic activity. Combining our present findings with our previous work (Cui et al., 2013), we propose that SU4312 concurrently possesses neuronal NOS inhibition, anti-oxidative stress, and MEF2D enhancement activities to exert neuroprotection in Parkinson's models.

5. Conclusion

In the current study, we provide direct evidence that the anticancer agent SU4312 protected PC12 cells from MPP^+-induced neuronal death, as well as reversed Parkinsonian motor defects from MPTP-induced neurotoxicity and partially prevented depletion of dopamine and its metabolites in mice, possibly through multiple mechanisms including enhancement of MEF2D through the activation of PI3-K/Akt pathway, maintenance of mitochondrial biogenesis and inhibition of MAO-B activity. SU4312 thus may be an effective drug candidate for the prevention or even modification of the pathological processes of PD.

Conflict of interest

The authors have no conflict of interest to declare.

Acknowledgments

This study was supported by grants from by the Natural National Science Foundation of China (NSFC 81303251; 81673407), the Natural Science Foundation of Guangdong Province (2015A030313317), the research grants from PolyU (G-YBGQ, G-YZ95), the Research Grants Council of Hong Kong (15101014), ITSP-Guangdong-Hong Kong Technology Cooperation Funding Scheme (GHP/012/16GD), Shenzhen Basic Research Program (JCYJ20160331141459373), China Postdoctoral Science Foundation Grant (2015M570753), and partially by grants from the Science and Technology Development Fund (FDCT) of Macao SAR (Ref. No. 134/2014/A3), Research Committee of University of Macau (MYRG2016-00129-ICMS-QRCM), and the Overseas and Hong Kong, Macau Young Scholars Collaborative Research Fund by the Natural National Science Foundation of China (81328025). We sincerely thank Ms. Josephine Leung for proofreading our manuscript.

References

Boll, M.C., Alcaraz-Zubeldia, M., Rios, C., 2011. Medical management of Parkinson's disease: focus on neuroprotection. Curr. Neuropharmacol. 9, 350–359.
Cacabelos, R., 2017. Parkinson's disease: from pathogenesis to pharmacogenomics. Int. J. Mol. Sci. 18.
Chen, Z.W., Liu, A., Liu, Q., Chen, J., Li, W.M., Chao, X.J., Yang, Q., Liu, P.Q., Mao, Z.X., Pi, R.B., 2016. MEF2D mediates the neuroprotective effect of methylene blue against glutamate-induced oxidative damage in HT22 hippocampal cells. Mol. Neurobiol. 54, 2209–2222.
Chu, Y., Mickiewicz, A.L., Kordower, J.H., 2011. alpha-synuclein aggregation reduces nigral myocyte enhancer factor-2D in idiopathic and experimental Parkinson's disease. Neurobiol. Dis. 41, 71–82.
Cramer, P.E., Cirrito, J.R., Wesson, D.W., Lee, C.Y., Karlo, J.C., Zinn, A.E., Casali, B.T., Restivo, J.L., Goebel, W.D., James, M.J., Brunden, K.R., Wilson, D.A., Landreth, G.E., 2012. ApoE-directed therapeutics rapidly clear beta-amyloid and reverse deficits in AD mouse models. Science 335, 1503–1506.
Cui, W., Zhang, Z., Li, W., Hu, S., Mak, S., Zhang, H., Han, R., Yuan, S., Li, S., Sa, F., Xu, D., Lin, Z., Zuo, Z., Rong, J., Ma, E.D., Choi, T.C., Lee, S.M., Han, Y., 2013. The anti-cancer agent SU4312 unexpectedly protects against MPP(+) -induced neurotoxicity via selective and direct inhibition of neuronal NOS. Br. J. Pharmacol. 168, 1201–1214.
Driver, J.A., 2014. Inverse association between cancer and neurodegenerative disease: review of the epidemiologic and biological evidence. Biogerontology 15, 547–557.
Finkelstein, D.I., Stanic, D., Parish, C.L., Drago, J., Horne, M.K., 2004. Quantified assessment of terminal density and innervation. Curr. Protoc. Neurosci. 13. Chapter 1, Unit 1.
Guo, B., Zheng, C., Cai, W., Cheng, J., Wang, H., Li, H., Sun, Y., Cui, W., Wang, Y., Han, Y., Lee, S.M., Zhang, Z., 2016. Multifunction of chrysin in Parkinson's model: anti-neuronal apoptosis, neuroprotection via activation of MEF2D, and inhibition of monoamine oxidase-B. J. Agric. Food Chem. 64, 5324–5333.
Hara, M.R., Thomas, B., Cascio, M.B., Bae, B.I., Hester, L.D., Dawson, V.L., Dawson, T.M., Sawa, A., Snyder, S.H., 2006. Neuroprotection by pharmacologic blockade of the GAPDH death cascade. Proc. Natl. Acad. Sci. U. S. A. 103, 3887–3889.
Hebron, M.L., Lonskaya, I., Moussa, C.E., 2013. Nilotinib reverses loss of dopamine neurons and improves motor behavior via autophagic degradation of alpha-synuclein in Parkinson's disease models. Hum. Mol. Genet. 22, 3315–3328.
Hu, S., Cui, W., Mak, S., Xu, D., Hu, Y., Tang, J., Choi, C., Lee, M., Pang, Y., Han, Y., 2015a. Substantial neuroprotective and neurite outgrowth-promoting activities by bis(propyl)-cognitin via the activation of Alpha7-nAChR, a promising anti-Alzheimer's dimer. ACS Chem. Neurosci. 6, 1536–1545.
Hu, S., Cui, W., Zhang, Z., Mak, S., Xu, D., Li, G., Hu, Y., Wang, Y., Lee, M., Tsim, K.W., Han, Y., 2015b. Indirubin-3-oxime effectively prevents 6OHDA-induced neurotoxicity in PC12 cells via activating MEF2D through the inhibition of GSK3beta. J. Mol. Neurosci. 57, 561–570.
Huang, L., Deng, M., He, Y., Lu, S., Liu, S., Fang, Y., 2016. beta-asarone increases MEF2D and TH levels and reduces alpha-synuclein level in 6-OHDA-induced rats via regulating the HSP70/MAPK/MEF2D/Beclin-1 pathway: chaperone-mediated autophagy activation, macroautophagy inhibition and HSP70 up-expression. Behav. Brain Res. 313, 370–379.
Karuppagounder, S.S., Brahmachari, S., Lee, Y., Dawson, V.L., Dawson, T.M., Ko, H.S., 2014. The c-Abl inhibitor, nilotinib, protects dopaminergic neurons in a pre-clinical animal model of Parkinson's disease. Sci. Rep. 4, 4874.
Lee, B.D., Shin, J.H., VanKampen, J., Petrucelli, L., West, A.B., Ko, H.S., Lee, Y.I., Maguire-Zeiss, K.A., Bowers, W.J., Federoff, H.J., Dawson, V.L., Dawson, T.M., 2010. Inhibitors of leucine-rich repeat kinase-2 protect against models of Parkinson's disease. Nat. Med. 16, 998–1000.
Mahul-Mellier, A.L., Fauvet, B., Gysbers, A., Dikiy, I., Oueslati, A., Georgeon, S., Lamontanara, A.J., Bisquertt, A., Eliezer, D., Masliah, E., Halliday, G., Hantschel, O., Lashuel, H.A., 2014. c-Abl phosphorylates alpha-synuclein and regulates its degradation: implication for alpha-synuclein clearance and contribution to the pathogenesis of Parkinson's disease. Hum. Mol. Genet. 23, 2858–2879.
Mandir, A.S., Przedborski, S., Jackson-Lewis, V., Wang, Z.Q., Simbulan-Rosenthal, C.M., Smulson, M.E., Hoffman, B.E., Guastella, D.B., Dawson, V.L., Dawson, T.M., 1999. Poly(ADP-ribose) polymerase activation mediates 1-methyl-4-phenyl-1, 2,3,6-tetrahydropyridine (MPTP)-induced parkinsonism. Proc. Natl. Acad. Sci. U. S. A. 96, 5774–5779.
Miki, A., Miki, K., Ueno, S., Wersinger, D.M., Berlinicke, C., Shaw, G.C., Usui, S., Wang, Y., Zack, D.J., Campochiaro, P.A., 2010. Prolonged blockade of VEGF receptors does not damage retinal photoreceptors or ganglion cells. J. Cell Physiol. 224, 262–272.
Mount, M.P., Zhang, Y., Amini, M., Callaghan, S., Kulczycki, J., Mao, Z., Slack, R.S., Anisman, H., Park, D.S., 2013. Perturbation of transcription factor Nur77 expression mediated by myocyte enhancer factor 2D (MEF2D) regulates dopaminergic neuron loss in response to 1-methyl-4-phenyl-1,2,3,6-tetrahydropyridine (MPTP). J. Biol. Chem. 288, 14362–14371.
Musicco, M., Adorni, F., Di Santo, S., Prinelli, F., Pettenati, C., Caltagirone, C., Palmer, K., Russo, A., 2013. Inverse occurrence of cancer and Alzheimer disease: a population-based incidence study. Neurology 81, 322–328.
Myllyla, V.V., Sotaniemi, K., Maki-Ikola, O., Rinne, U.K., Heinonen, E.H., 1996. Role of selegiline in combination therapy of Parkinson's disease. Neurology 47,

S200–S209.
Okamoto, S., Nakamura, T., Cieplak, P., Chan, S.F., Kalashnikova, E., Liao, L., Saleem, S., Han, X., Clemente, A., Nutter, A., Sances, S., Brechtel, C., Haus, D., Haun, F., Sanz-Blasco, S., Huang, X., Li, H., Zaremba, J.D., Cui, J., Gu, Z., Nikzad, R., Harrop, A., McKercher, S.R., Godzik, A., Yates 3rd, J.R., Lipton, S.A., 2014. S-nitrosylation-mediated redox transcriptional switch modulates neurogenesis and neuronal cell death. Cell Rep. 8, 217–228.
Pon, J.R., Marra, M.A., 2016. MEF2 transcription factors: developmental regulators and emerging cancer genes. Oncotarget 7, 2297–2312.
Qiao, C., Zhang, L.X., Sun, X.Y., Ding, J.H., Lu, M., Hu, G., 2017. Caspase-1 deficiency alleviates dopaminergic neuronal death via inhibiting caspase-7/AIF pathway in MPTP/p mouse model of Parkinson's disease. Mol. Neurobiol. 54, 4292–4302.
Rascol, O., Lozano, A., Stern, M., Poewe, W., 2011. Milestones in Parkinson's disease therapeutics. Mov. Disord. 26, 1072–1082.
Rashid, A.J., Cole, C.J., Josselyn, S.A., 2014. Emerging roles for MEF2 transcription factors in memory. Genes Brain Behav. 13, 118–125.
Rojas, R.J., Edmondson, D.E., Almos, T., Scott, R., Massari, M.E., 2015. Reversible and irreversible small molecule inhibitors of monoamine oxidase B (MAO-B) investigated by biophysical techniques. Bioorg. Med. Chem. 23, 770–778.
Sagi, Y., Mandel, S., Amit, T., Youdim, M.B., 2007. Activation of tyrosine kinase receptor signaling pathway by rasagiline facilitates neurorescue and restoration of nigrostriatal dopamine neurons in post-MPTP-induced parkinsonism. Neurobiol. Dis. 25, 35–44.
She, H., Yang, Q., Shepherd, K., Smith, Y., Miller, G., Testa, C., Mao, Z., 2011. Direct regulation of complex I by mitochondrial MEF2D is disrupted in a mouse model of Parkinson disease and in human patients. J. Clin. Invest. 121, 930–940.
Smith, P.D., Mount, M.P., Shree, R., Callaghan, S., Slack, R.S., Anisman, H., Vincent, I., Wang, X., Mao, Z., Park, D.S., 2006. Calpain-regulated p35/cdk5 plays a central role in dopaminergic neuron death through modulation of the transcription factor myocyte enhancer factor 2. J. Neurosci. 26, 440–447.
Sun, L., Tran, N., Tang, F., App, H., Hirth, P., McMahon, G., Tang, C., 1998. Synthesis and biological evaluations of 3-substituted indolin-2-ones: a novel class of tyrosine kinase inhibitors that exhibit selectivity toward particular receptor tyrosine kinases. J. Med. Chem. 41, 2588–2603.
Tabares-Seisdedos, R., Rubenstein, J.L., 2013. Inverse cancer comorbidity: a serendipitous opportunity to gain insight into CNS disorders. Nat. Rev. Neurosci. 14, 293–304.
Tanabe, A., Yamamura, Y., Kasahara, J., Morigaki, R., Kaji, R., Goto, S., 2014. A novel tyrosine kinase inhibitor AMN107 (nilotinib) normalizes striatal motor behaviors in a mouse model of Parkinson's disease. Front. Cell Neurosci. 8, 50.
Tieu, K., 2011. A guide to neurotoxic animal models of Parkinson's disease. Cold Spring Harb. Perspect. Med. 1, a009316.
Tran, T., Sneed, B., Haider, J., Blavo, D., White, A., Aiyejorun, T., Baranowski, T.C., Rubinstein, A.L., Doan, T.N., Dingledine, R., Sandberg, E.M., 2007. Automated, quantitative screening assay for antiangiogenic compounds using transgenic zebrafish. Cancer Res. 67, 11386–11392.
Trinh, J., Farrer, M., 2013. Advances in the genetics of Parkinson disease. Nat. Rev. Neurol. 9, 445–454.
Wang, X., She, H., Mao, Z., 2009. Phosphorylation of neuronal survival factor MEF2D by glycogen synthase kinase 3beta in neuronal apoptosis. J. Biol. Chem. 284, 32619–32626.
Weinreb, O., Amit, T., Bar-Am, O., Sagi, Y., Mandel, S., Youdim, M.B., 2006. Involvement of multiple survival signal transduction pathways in the neuroprotective, neurorescue and APP processing activity of rasagiline and its propargyl moiety. J. Neural Transm. Suppl. 457–465.
Weinreb, O., Amit, T., Bar-Am, O., Youdim, M.B., 2010. Rasagiline: a novel anti-Parkinsonian monoamine oxidase-B inhibitor with neuroprotective activity. Prog. Neurobiol. 92, 330–344.
Wrasidlo, W., Crews, L.A., Tsigelny, I.F., Stocking, E., Kouznetsova, V.L., Price, D., Paulino, A., Gonzales, T., Overk, C.R., Patrick, C., Rockenstein, E., Masliah, E., 2014. Neuroprotective effects of the anti-cancer drug sunitinib in models of HIV neurotoxicity suggests potential for the treatment of neurodegenerative disorders. Br. J. Pharmacol. 171, 5757–5773.
Wu, R.M., Chen, R.C., Chiueh, C.C., 2000. Effect of MAO-B inhibitors on MPP+ toxicity in Vivo. Ann. N. Y. Acad. Sci. 899, 255–261.
Yang, Q., She, H., Gearing, M., Colla, E., Lee, M., Shacka, J.J., Mao, Z., 2009. Regulation of neuronal survival factor MEF2D by chaperone-mediated autophagy. Science 323, 124–127.
Yao, L., Li, W., She, H., Dou, J., Jia, L., He, Y., Yang, Q., Zhu, J., Capiro, N.L., Walker, D.I., Pennell, K.D., Pang, Y., Liu, Y., Han, Y., Mao, Z., 2012. Activation of transcription factor MEF2D by bis(3)-cognitin protects dopaminergic neurons and ameliorates Parkinsonian motor defects. J. Biol. Chem. 287, 34246–34255.